Engineering Science & Technology
http://ojs.wiserpub.com/index.php/EST/

Research Article

Studies Based on CFD Behaviour of Aerofoil and Regression Analysis

Satish Geeri*, Sambhu Prasad Surapaneni, Jithendra Sai Raja Chada, Akhil Yuvaraj Manda

Department of Mechanical Engineering, Pragati Engineering College, Surampalem, Andhra Pradesh, India
Email: geerisatish@gmail.com

Received: 28 August 2021; **Revised:** 30 September 2021; **Accepted:** 15 October 2021

Abstract: The performance of an aerofoil depends upon the angle of attack, leading-edge radius, surface modifications, etc. The aerofoil, which has a broader range of attack angle and surface area, is responsible for the upliftment in the performance of the aerofoil. The present work deals with the evaluation of the aerofoil spread with dimples over the active surface. The positions and areas of spread are modified accordingly and evaluated for the velocity and pressure lineation. The aerofoil with 30% dimples over the active surface is found to possess higher values for the required intents of velocity and pressure at an inlet velocity of 9 m/s. The optimum model with better lineation values is further evaluated for the coefficients of lift and drag to propose the best design. The best result is obtained at an aerofoil of NACA 8412 series with a 30% dimple extension at the rear end, placed at 15° angle of attack, and the regression analysis is done for the coefficient of lift values.

***Keywords*:** aerofoil, active surface, k-epsilon energy equation, fluent software, auto CAD software

1. Introduction

An aerofoil is a shaped body designed to move against a force using the aerodynamic force which is generated along the surface. The design of the aerofoil is the most crucial element in the efficiency of the aerofoil. The aerofoils are the rotating blades of a steam turbine that possess minimal weight, durable nature, offer better performance, efficiency in working, etc. When the aerofoil is allowed to move through the fluid, it generates an aerodynamic force which is essential in providing a characteristic shape to work with more efficiency.

Jithendra Sai Raja Chada et al. have studied the effect of the shape of dimples and arrangement of dimples on the surface of the aerofoil. The flow analysis on the aerofoil with circular and triangular dimples placed above the surface and both above & below the surface have concluded that the aerofoil with circular dimples above and below the surface shows better results [1]. Akhil Yuvaraj Manda et al. have studied the flow separation on NACA 6412, 7412, and NACA 8412 aerofoils by varying the angle of attack and inlet velocity. It is found that the aerofoil NACA 8412 has shown better results at an inlet velocity of 9 m/s [2]. Prasath M. S. et al. have studied the effect of dimples on the active surface of the aerofoil. The study concluded that the dimples convert the boundary layer from laminar to turbulent. This leads to reducing in drag forces [3]. T. H. New et al. have studied the effect of conjugations on the surface of the aerofoil and concluded that it consistently produces the best flow separation control characteristics [4]. Kirubakar K. et al. have studied the flow on a flat plate, aerofoil, and aerofoil with the enhanced surface to conclude that the enhanced surface

DOI: https://doi.org/10.37256/est.3120221121

has shown a better L/D ratio [5].

Sandesh K. Rasal et al. have studied the performance of aerofoil with dimples on the upper surface. The dimples on the upper surface have shown higher lift to drag ratio compared to aerofoil with a regular surface [6]. Tulus et al. have studied the behaviour of aerofoil in a fluid medium using the Navier-Stokes equation. The Navier-Stokes equations are commonly used in describing the motion of fluids in models relevant to weather, ocean currents, water flow in pipes, and so forth [7]. H. Johari et al. have studied the aerofoil with leading-edge modifications. It is found that the modifications on the leading-edge cause grater flow separation compared with regular aerofoil [8]. Omkar Bhatkar et al. have studied the flow on a multi element aerofoil. It has been declared that in a chambered aerofoil the small change in parameters causes changes in flow lift and drag [9]. Yang Zhang et al. have studied the aerodynamic characteristics of different aerofoils. The coefficient of lift increases up to a certain angle of attack called critical angle of attack. After this, the lift coefficient decreases by increasing the angle of attack [10]. Mohamed A. Fouad Kandil et al. have studied the flow on GOE-387 aerofoil and concluded that a negative pressure coefficient is observed on the upper surface of the aerofoil and positive on the lower side of the aerofoil. This causes the lift force on the aerofoil [11]. Mohamed A. Fouad Kandil et al. have studied the lift and drag characteristics of GOE-387 aerofoil. It has been concluded that the increase in the angle of attack leads to an increase in drag force and drag coefficient [12]. Mayurkymar Kevadiya et al. have studied the coefficient of pressure on NACA 4412. As the angle of attack increases, the pressure coefficient value increases on the lower surface and decreases on the upper surface [13].

Justin Winslow et al. have studied the flow of aerofoil by varying the angle of attack. It is stated that as the angle of attack increases, the turbulence increases on the active surface [14]. N. Cao et al. have studied the lift and drag characteristics of an aerofoil structure experimentally. The lift value increases by increasing the angle of attack and turbulence on the active surface. After reaching a peak value, the lift decreases and suggesting that the initiation of separation points of the boundary layer from the trailing edge towards the leading-edge takes place [15]. Livya et al. have studied the flow of aerofoil with different shapes of dimples. The dimples have reduced the coefficient of drag compared to the plain aerofoil [16]. Deepanshu Srivastav et al. have studied the effect of the shape of the dimple on the flow over an aerofoil. The study has concluded that the spherical-shaped dimples have shown better lift [17]-[20].

Based on the previous works, very little literature is available in terms of analysis of active surface region on the aerofoil. The present work elaborates on the process of finding out an optimum and perfect design to obtain maximum and appreciable efficiency. The work intends to design an aerofoil geometry with surface modifications that are evaluated based on velocity lineation, pressure lineation, dimple's location, dimples extension, and angle of attack. The final accomplishment is an aerofoil geometry based on the mentioned conditions and applications.

2. Detailed procedure

The aerofoil geometry of series NACA 8412 possesses the best performance at an inlet velocity of 9 m/s [1]. The geometry is placed at normal along the x-axis with a total of 81 plot points. The geometry is generated using the plot points using the AUTODESK-AUTOCAD software. The plotted geometry is applied with surfaces and modified with dimples over the active surface; thereby analyzed for the simulation using the SOLIDWORKS software. The base geometry of the aerofoil of the NACA 8412 series is shown in Figure 1. The geometry is modified accordingly in terms of the percentage of dimples spread over the active surface ranging from 10% to 100% with 10% intervals as shown in Figure 2 for 30% to the chord length of the upper surface. The value of the inlet velocity is maintained to be constant at 9 m/s.

The finalized geometry is designed and is evaluated in a predefined procedure as mentioned. The geometry is applied with principles such as Bernoulli's equation and Navier-Stokes equation by varying the angle of attack with an interval of 5°. The evaluation with regard to the calculation is termed as follows.

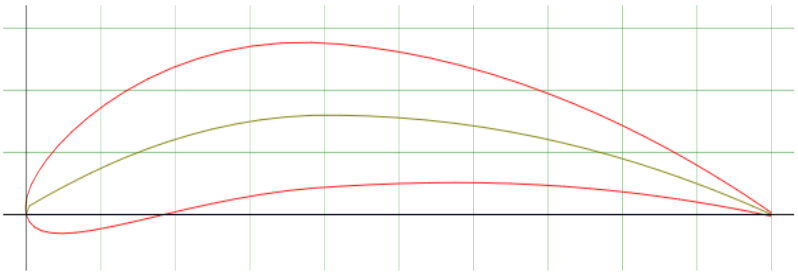

Figure 1. Reference plot of NACA 8412 series without dimples

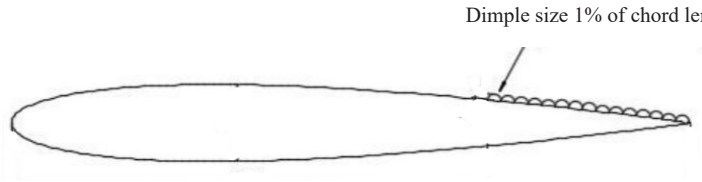

Figure 2. Aerofoil with dimples of 30% to the chord length

2.1 *Bernoulli's equation*

The application of principle between the principle of conservation of energy leads to a relation between the pressure and velocity of the flow in a fluid. This relation is called Bernoulli's Equation.

$$\text{Work done} = \text{Kinetic Energy} + \text{Potential Energy} \tag{1}$$

$$\Delta W = \Delta(KE + PE)$$

Work done equals force multiplied by distance:

$$W = Fd \tag{2}$$

We can plug in the formula that relates pressure and force, which gives us:

$$W = pAd \tag{3}$$

Where A represents area.
Volume is derived by multiplying area and height (distance), thus:

$$W = pV \tag{4}$$

Work done is equal to:

$$\Delta W = P_1V_1 - P_2V_2 \tag{5}$$

Kinetic energy is the energy of mass in motion:

$$KE = \frac{mv_2}{2} = \frac{pVv_2}{2} \tag{6}$$

Where V represents volume.
Potential energy is dependent on height:

$$PE = mgy = \rho Vgy$$

Where y represents height.
Substituting gives:

$$P_1V - P_2V = \frac{\rho Vv_2^2}{2} + \rho Vgy_2 - \frac{\rho Vv_1^2}{2} - \rho Vgy_1 \tag{7}$$

Divide by V:

$$P_1 - P_2 = \frac{\rho v_2^2}{2} + \rho gy_2 - \frac{\rho v_1^2}{2} - \rho gy_1$$

Rearranging the formula to put the terms that refer to the same point on the same side of the equation:

$$P_1 + \frac{1}{2}\rho v_1^2 + \rho gy_1 = P_2 + \frac{1}{2}\rho v_2^2 + \rho gy_2 \tag{8}$$

2.2 *Navier-Stokes equation*

Navier-Stokes equation acts as a base principle for all the CFD flow modelling and evaluations. The Navier-Stokes equation also acts as the conservation of momentum principle. The final equation is represented as mentioned.

$$\rho\frac{\delta v}{\delta t} = -\nabla p + \rho g + \mu\nabla 2v \tag{9}$$

Where, ρ = fluid density.
v = fluid flow velocity.
p = fluid pressure.
μ = fluid dynamic viscosity.
∇ = del operator.

3. Results and discussion

The intent of the work is to elaborate and evaluate an optimum aerofoil geometry with efficient values in all the possible cases. The simulations and evaluations are carried out using the SOLIDWORKS software. The aerofoil geometry is first altered with the addition of dimples over the surface at various positions. The appreciable geometry with arrangement at a fixed area is further evaluated for the extension of dimples over the active surface. The optimum aerofoil with further evaluations is opted and is altered in terms of angle of attack and thereby is evaluated in terms of performance along with the coefficient of lift and drag. The conception and evaluation are termed and proceeded as discussed.

3.1 *Location of dimple*

The aerofoil geometry of NACA 8412 series has been elaborated and evaluated for different conditions possible [2]. The aerofoil geometry is modified by adding some spherical-shaped structures known as dimples over the active surface at various proportions [1]. These dimples are altered accordingly at three different positions such as front, middle, and rear. These designed models with dimples at various positions are evaluated for the outlet velocity lineation and outlet pressure lineation at an inlet velocity of 9 m/s [2]. The results obtained show that the maximum values can be gained by placing the dimples at the rear end of the aerofoil geometry [1].

Table 1. Lineation values of the dimples positioning

Lineation	Description	At front	At middle	At rear
Velocity (m/s)	Min outlet velocity	-1.921	-1.577	0
	Max outlet velocity	10.809	10.733	10.899
Pressure (Pa)	Min outlet pressure	101,281.3	101,271.4	101,271.368
	Maximum outlet pressure	101,381.2	101,378.3	101,378.158

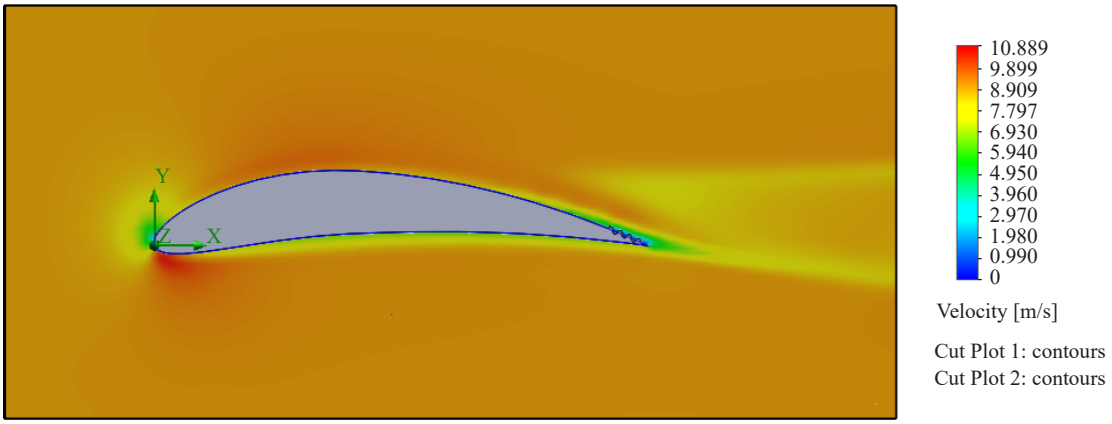

Figure 3. Reference plot of NACA 8412 series without dimples

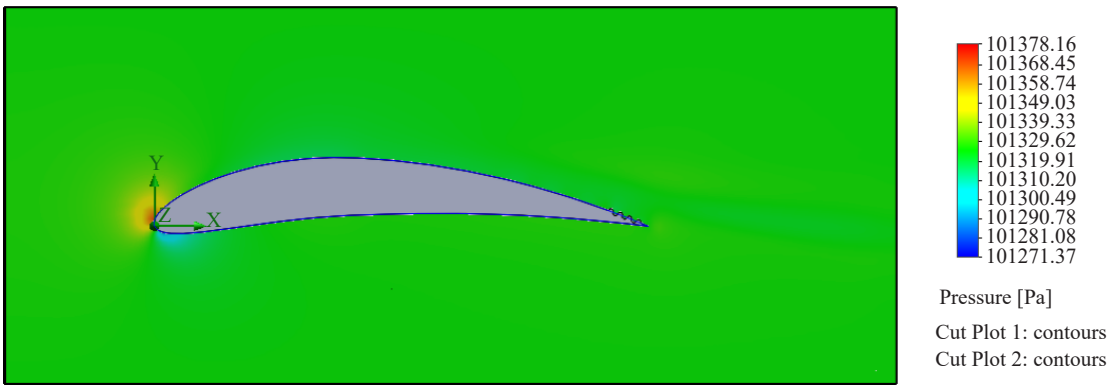

Figure 4. Reference plot of NACA 8412 series without dimples

The tabular results represent the simulation values for the outlet velocity and outlet pressure lineation when the dimples are placed at different locations as shown in Table 1. The maximum values in terms of both lineations can be observed at the rear end of the aerofoil. The aerofoil when modified at the rear end of the geometry contributes to the negative pressure to develop along the corner. This negative pressure contributes to the increase in the values of the velocity and pressure lineation values, thereby making it the optimum position to allow for the arrangement of the dimples. Figure 3 displays the velocity lineation when the dimples are placed at the rear end; whereas Figure 4 displays the pressure lineation when the dimples are placed at the rear end. The maximum outlet velocity obtained is 10.899 m/s at the rear end; whereas the lowest velocity is 10.809 m/s at the front end. The velocity lineation increased by 17.7% by placing the dimples at the rear end when compared to the other two positions. The maximum outlet pressure developed was 101,381.2 at the front end of the aerofoil geometry.

3.2 *Dimple span from the rear end of aerofoil*

Results based on the 3.1 section, depicted that the aerofoil geometry exhibited the best values when the dimples are placed at the rear end, the further simulations and evaluations are carried out under the same conditions of placing the dimples at the rear end and an inlet velocity of 9 m/s. The arrangement of dimples is extended from a range of 10% to 100% spread of dimples over the active surface. The lineation when plotted as a graph depicted maximum deviation at 30% spread of dimples over the active surface of the aerofoil as shown in Figure 5. The ratio of the coefficient of lift to the coefficient of drag (C_l/C_d) values is maximum for the 30% dimple span from the rear end of aerofoil as represented in Table 2.

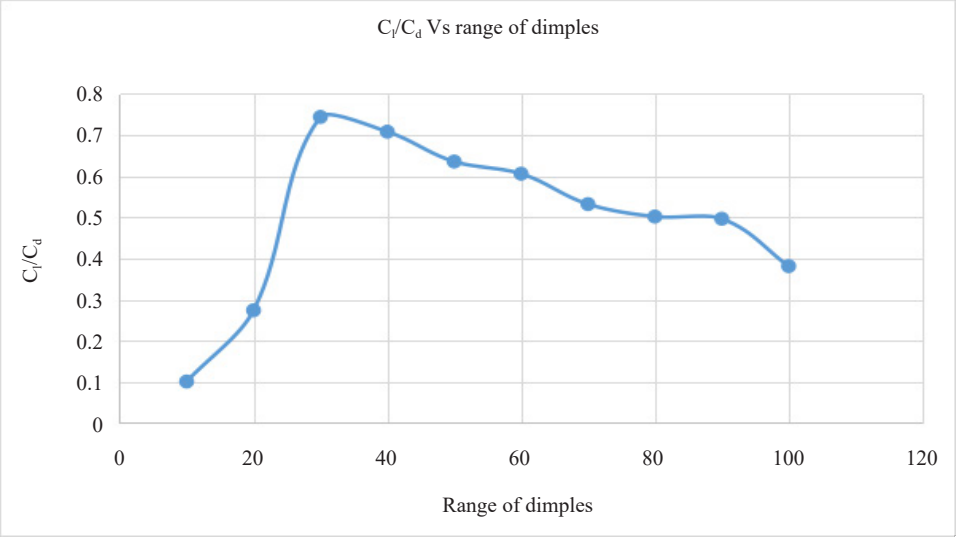

Figure 5. Plot for variation in the spread of dimples

The results are plotted for the co-efficient of lift and drag against the range of dimples spread over the active surface of the aerofoil as shown in Figure 6. The maximum deviation can be found when the dimples are spread around 30% over the active surface as shown in Figure 5. It led to an appreciable increase in terms of the coefficient of lift and coefficient of drag. There is a remarkable difference of about 63.9% deviation at that value of 30% extensions of dimples.

Table 2. C_l/C_d values for extension of dimples

Extension of dimples	C_l/C_d
10%	0.101
20%	0.274020937
30%	0.74392272
40%	0.708045817
50%	0.635455527
60%	0.605844656
70%	0.53211246
80%	0.501792682
90%	0.496556509
100%	0.381383059

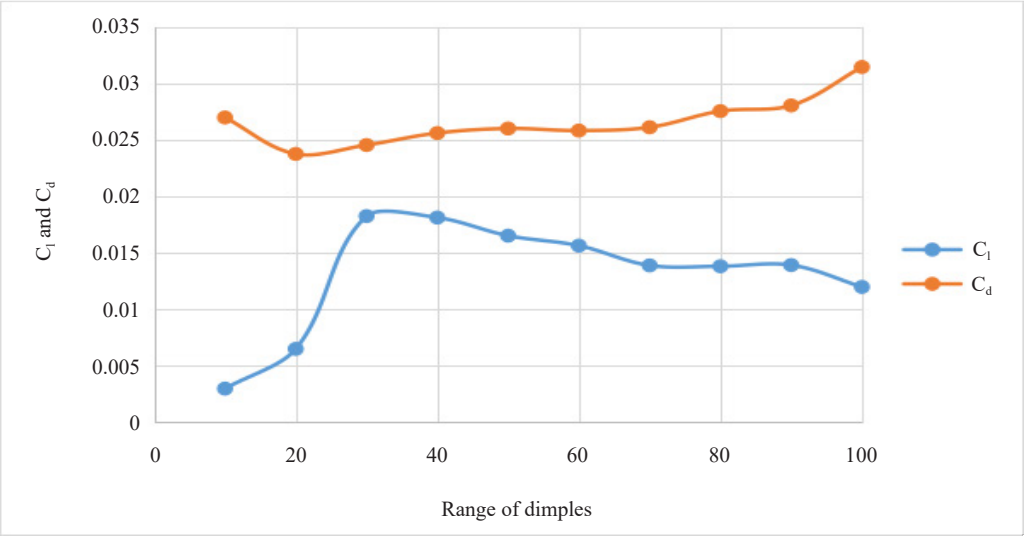

Figure 6. The variation of lift and drag coefficient with the spread of dimples

As the arrangement of dimples contributes to an increase in the efficiency of the aerofoil, the number of dimples spread over the surface also possesses a major impact on it. The best value is depicted on comparing with the C_l/C_d ratio as shown in Figure 5. The tabular results (Table 2) also depict the best value with maximum deviation at 30% extension, thereby affirming it as the best value. Figures 7-8 display the velocity lineation and pressure lineation for the aerofoil geometry arranged with 30% dimples extension on the rear end. The maximum outlet velocity of 10.886 m/s is also obtained at 30% extension and the maximum outlet pressure of 101,378.418 Pa is also obtained at 30% extension of dimples over the active surface. Due to the pressure differences and the velocity going over the active surface, it contributes to the variations in the lift force [1], [13], [15].

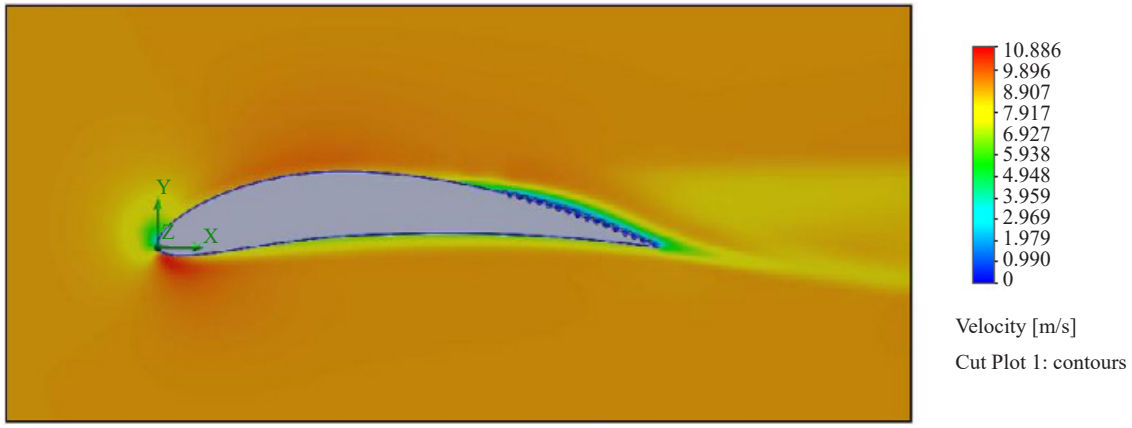

Figure 7. Velocity lineation to 30% dimpled aerofoil

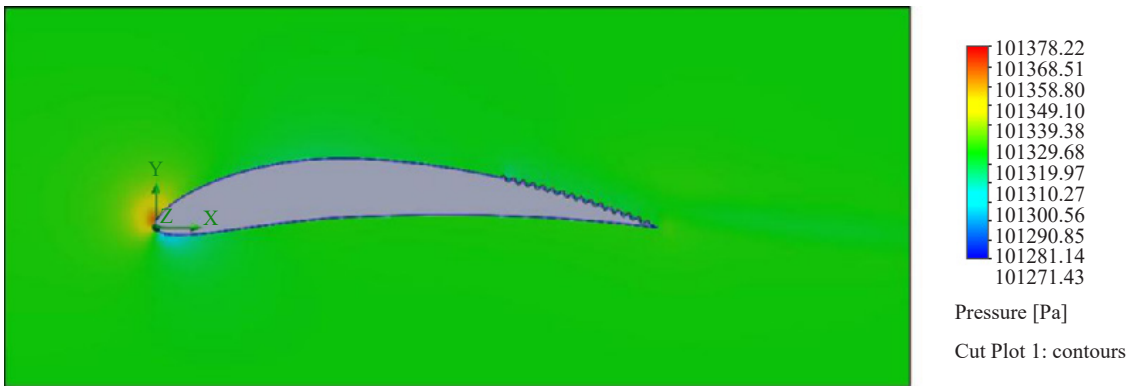

Figure 8. Pressure lineation to 30% dimpled aerofoil

3.3 *Impact by the angle of attack*

With reference to the 3.2 section, depicted that the aerofoil geometry arranged with dimples at the rear end with 30% spread over the active surface is an optimum design. Therefore, further evaluations are carried out to find an optimum angle of attack to place the aerofoil at a fixed constrain. The aerofoil with 30% dimples at the rear end is evaluated by altering the angle of attack from 0°-60° with a 5° interval as shown in Figures 9-10. Based on Figure 9, the coefficient of drag value is gradually improved as the angle of attack is increased. A similar trend is mentioned in the previous work as the attack angle increases, the drag force, and drag coefficient also increase [12].

Figure 9 also represents the coefficient of lift value increases up to 50° of the angle of attack and later it drops. As the angle of attack approaches 50°, it reaches a critical angle of attack and it has a major influence on the C_l/C_d ratio [10], [15], [21] and this C_l/C_d ratio is one of the parameters which is influenced on the performance of the aerofoil. The maximum impact in terms of C_l/C_d is observed at an angle of 15° as shown in Figure 10. The results plotted to depict an appreciable and large amount of deviation at an angle of 15°.

The peak value is observed at a 15° angle of attack in terms of the C_l/C_d ratio. When the angle of attack is altered, the negative pressure gets developed. This negative pressure developed gets neutralized or gets canceled by the drag force generated behind the aerofoil geometry. This cancellation between the drag force and the pressure leads to consideration of the lift force. Table 3 displays the C_l/C_d ratio and coefficient of lift values where maximum values are observed at 15° and 50° thereby affirming it as the optimum angle of attack.

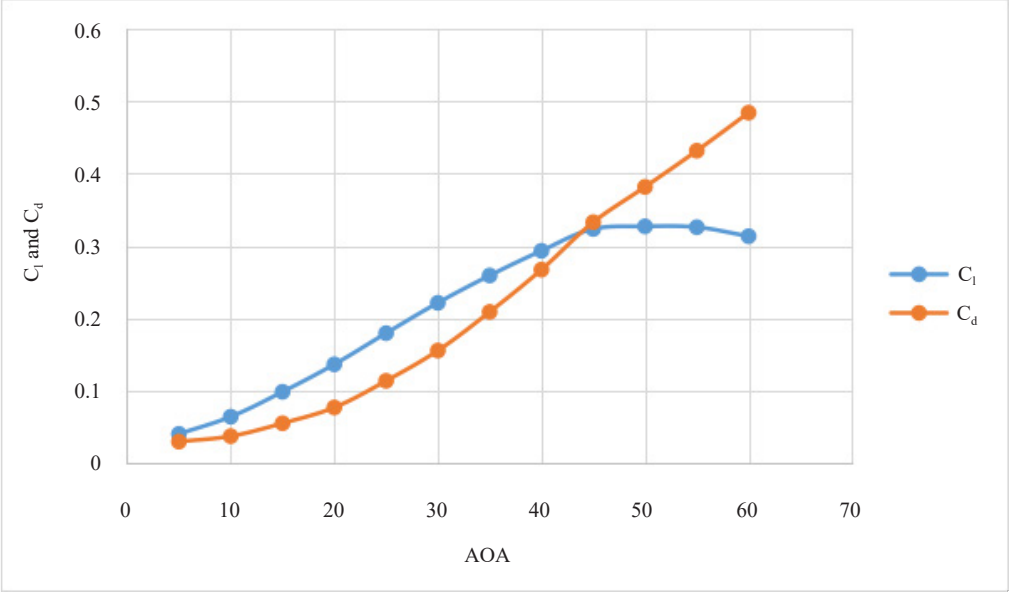

Figure 9. The variation of lift and drag coefficient with angle of attack

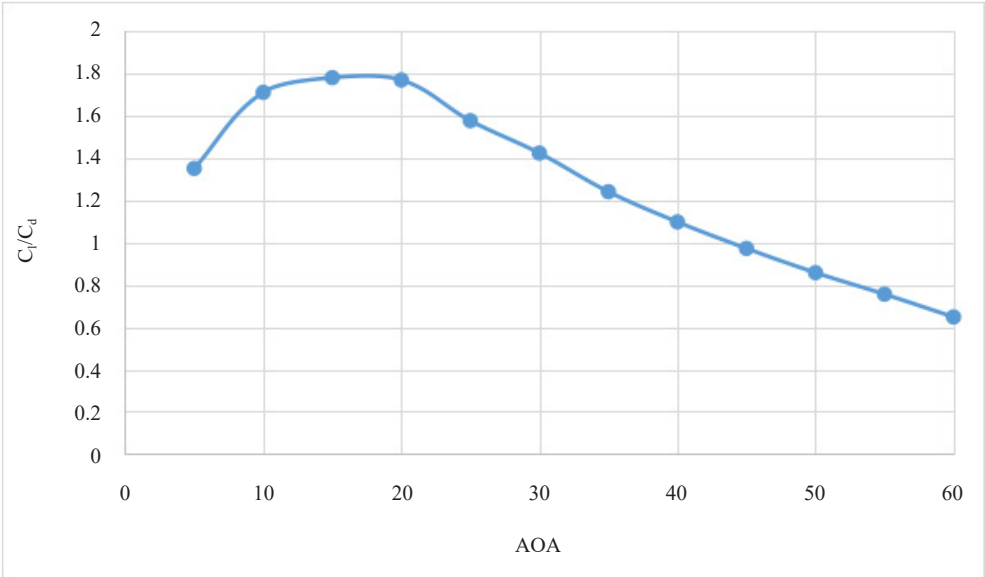

Figure 10. C_l/C_d ratio to angle of attack

The main factor which contributes to the performance of the aerofoil is the lift force. The C_l/C_d ratio which is the most crucial and ultimate factor for deciding the optimum aerofoil is found to be 1.779177765. Figures 11 & 12 displays the velocity lineation and pressure lineation respectively for the aerofoil geometry with 30% dimples extension on the rear end placed at a 15° angle of attack. The maximum outlet velocity lineation of 12.179 m/s is observed at a 60° angle of attack but with a minimum deviation. The maximum outlet pressure of 101,412.71 Pa is also obtained at a 60° angle of attack.

Table 3. Co-efficient of lift and C_l/C_d ratio at various angles of attack

Angle of attack	C_l	C_l/C_d ratio
5°	0.041000059	1.35023846
10°	0.06473272	1.709700667
15°	0.09907801	1.779177765
20°	0.13699511	1.768112329
25°	0.179981444	1.575779546
30°	0.221905223	1.422542314
35°	0.259583065	1.240174202
40°	0.2936595	1.097247712
45°	0.32374997	0.971996138
50°	0.32740994	0.857509123
55°	0.32623343	0.755710165
60°	0.31377414	0.647989804

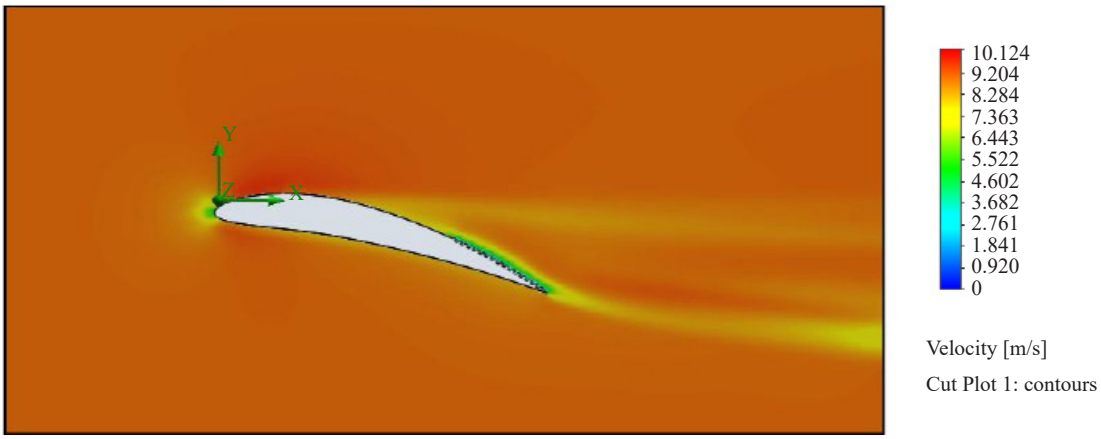

Figure 11. Velocity lineation to 30% dimpled aerofoil with 15° AOA

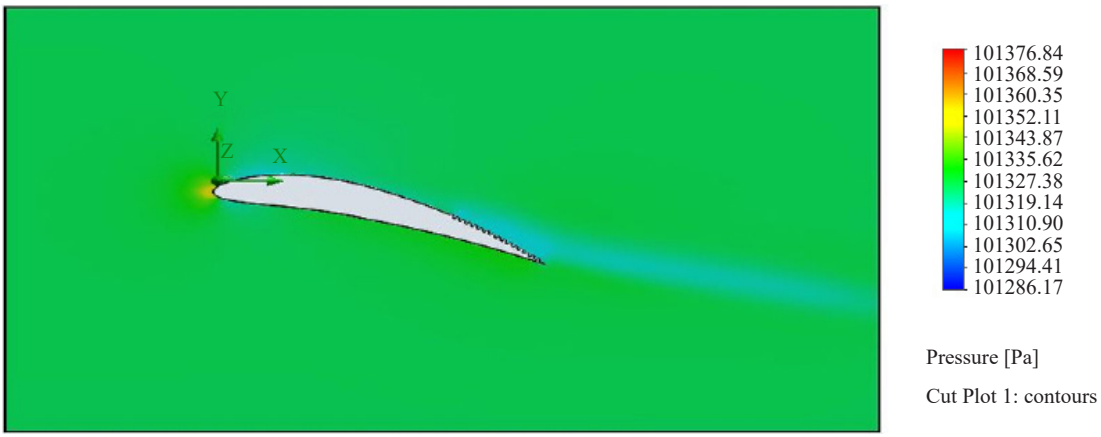

Figure 12. Pressure lineation to 30% dimpled aerofoil with 15° AOA

3.4 *Regression analysis*

Regression analysis is one of the simple techniques for finding the functional relationship among the variables and the influence of the variables on the response. This analysis is done in the Mini Tab software. The relation among the variables and the response will be generated based on the equation [19].

A mathematical model is generated by using the regression analysis as equation 10. The developed equation is based on simulated data by considering the response as the coefficient of lift and the dependant variable as angle of attack. In regression analysis, the R^2 value decides the accuracy level and the value is 99.9% and 97.9% as shown in Figures 13 & 14. Based on Figures 13 & 14, it is clear that the simulated data is exactly fit to curve. Hence it also explains the accuracy level of the simulated data generated in Ansys software.

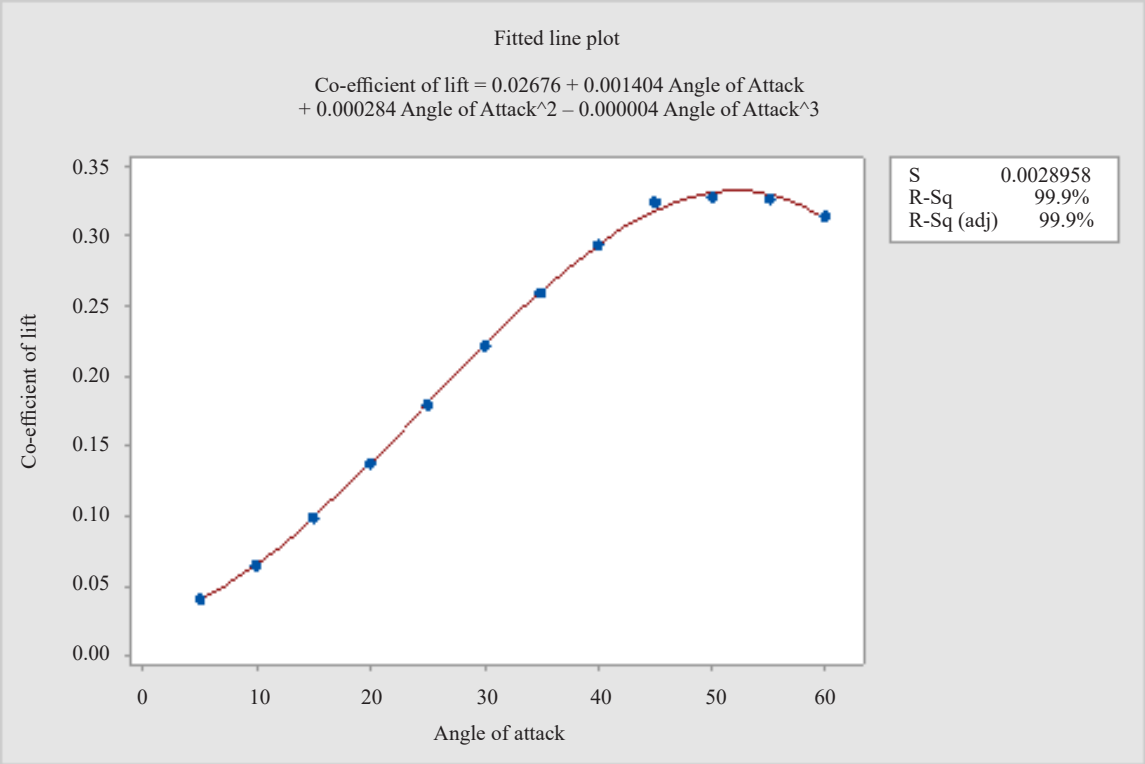

Figure 13. Simulated data Coefficient of lift (C_l) fitted to mathematical curve

The regression equation is:

$$\text{Coefficient of lift} = 0.02676 + (0.001404 \times \text{Angle of Attack})$$

$$+ (0.000284 \times (\text{Angle of Attack}^2)) - (0.000004 \times (\text{Angle of Attack}^3)) \quad (10)$$

S = 0.0028958.
R-Sq = 99.9%.
R-Sq (adj) = 99.9%.

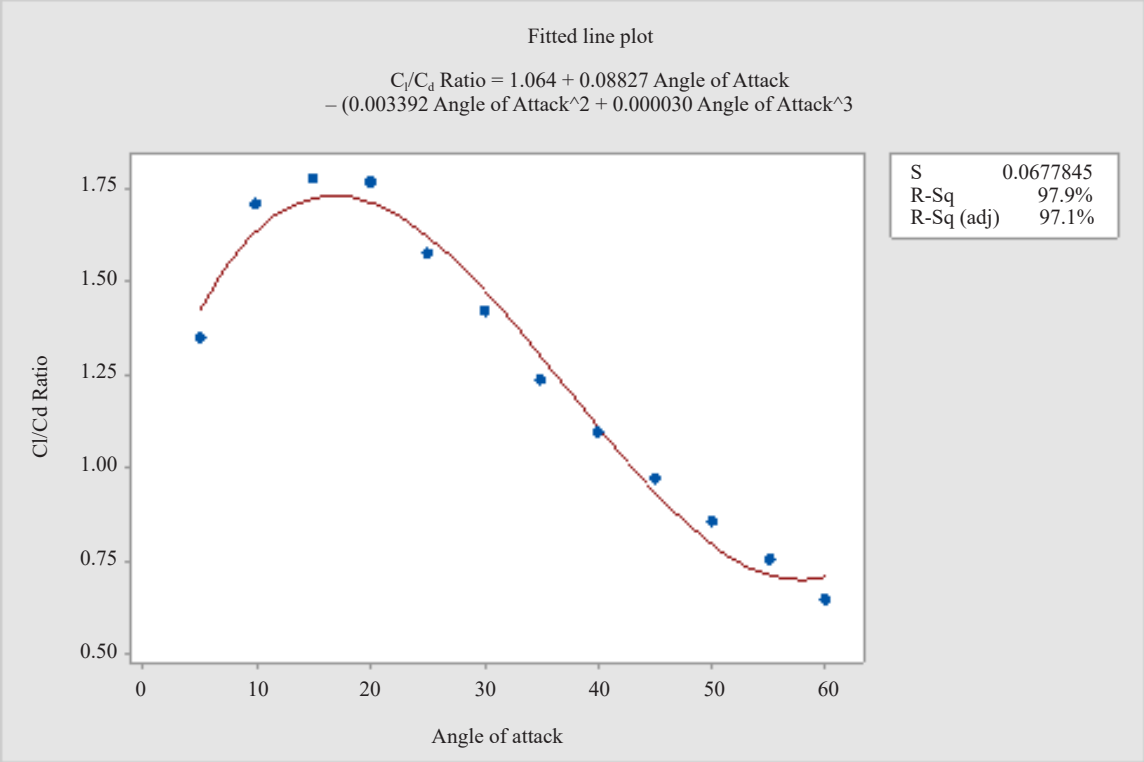

Figure 14. Simulated data Coefficient of lift (C_l) to Coefficient of drag (C_d) ratio fitted to mathematical curve

The regression equation is:

$$C_l/C_d \text{ Ratio} = 1.064 + (0.08827 \times (\text{Angle of Attack})) - (0.003392 \times (\text{Angle of Attack})^2) + (0.000030 \times (\text{Angle of Attack})^3) \quad (11)$$

S = 0.0677845.
R-Sq = 97.9%.
R-Sq (adj) = 97.1%.

5. Conclusions

The present work highlights the evaluation of the flow behavior over the surface of an aerofoil with dimples spread at the rear end of the geometry. The intent is to generate an aerofoil geometry with optimum values in terms of all the possible conditions. The aerofoil geometry is analyzed for the velocity lineation, pressure lineation, coefficient of lift, and coefficient of drag. The geometry is modified by a change in the number of dimples over the surface i.e., 10% to 100% with an interval of 10%. The modified geometry is evaluated with regard to the velocity lineation, pressure lineation, C_l/C_d ratio. The best values are obtained for 30% extension of dimples over the surface. This aerofoil geometry with 30% extension is further simulated, evaluated, and analyzed for various angles of attack. The final result surmised from all the results and evaluations is an aerofoil of the NACA 8412 series with 30% dimples extension on the active surface placed at a 15° angle of attack. The coefficient of lift to coefficient of drag ratio in the final simulation is found to have an increase by 51.37% by placing at 15° rather than placing at the normal. This appreciable increase under of all the applicable conditions makes it the optimum design of the aerofoil geometry. The simulated value of the coefficient of lift is in good fit and with high accuracy to the mathematical model equation.

Conflict of interest

The authors declare no conflict of interest.

References

[1] J. S. R. Chada, K. V. V. Satyanarayana, G. V. Kumar, M. Shaheen, and A. P. Bhaskar, ‘‘Flow analysis on aerofoil with surface modifications,’’ *I-manager's Journal on Mechanical Engineering*, vol. 10, no. 3, 2018.

[2] A. Y. Manda, J. S. R. Chada, S. P. Surapaneni, and S. Geeri, ‘‘Flow behaviour on aerofoils using CFD,’’ *Journal of Mechanical Engineering, Automation and Control Systems, JVE International*, vol. 1, no. 1, pp. 26-36, 2020.

[3] M. S. Prasath and A. S. Irish, ‘‘Effect of dimples on aircraft wing,’’ *Global Research and Development Journal for Engineering*, vol. 2, no. 5, pp. 234-242, 2017.

[4] T. H. New, Y. X. Chan, G. C. Koh, M. C. Hoang, and S. X. Shi, ‘‘Effects of corrugated aerofoil surface features on flow separation control,’’ *AIAA Journals*, vol. 52, no. 1, pp. 206-211, 2014.

[5] K. Kirubakar, P. Gayathri, V. Sindhuja, A. Senthamilselvi, ‘‘Design and analysis of corrugated wing section,’’ *SSRG International Journal of Mechanical Engineering*, no. ICTER, pp. 1-5, 2019.

[6] S. K. Rasal and R. R. Katwate, ‘‘Numerical analysis of lift & drag performance of NACA 0012,’’ *International Research Journal of Engineering and Technology*, vol. 4, no. 6, pp. 2892-2896, 2017.

[7] K. C. Tulus and S. Marpaung, ‘‘Computational analysis of fluid behaviour around airfoil with navier stokes equation,’’ *Journal of Physics: Conference Series*, pp. 1-8, 2018.

[8] H. Johari, C. Henoch, D. Custodio, and A. Levshin, ‘‘Effects of leading-edge protuberances on airfoil performances,’’ *AIAA Journals*, vol. 45, no. 11, pp. 2634-2642, 2007.

[9] O. Bhatkar, N. Prabhutendolkar, A. Sakpal, S. Sawant, and O. Sakpal, ‘‘2D analysis of multi-element airfoil for wing,’’ *International Research Journal of Engineering and Technology*, vol. 5, no. 2, pp. 174-177, 2018.

[10] Y. Zhang, Z. Zhou, K. L. Wang, and X. Li, ‘‘Aerodynamic characteristics of different airfoils under varied turbulent intensities at low Reynolds number,’’ *Applied Sciences*, vol. 10, pp. 2-19, 2020.

[11] M. A. F. Kandil and A. O. Elnady, ‘‘Performance of GOE-387 airfoil using CFD,’’ *International Journal of Aerospace Sciences*, vol. 5, no. 1, pp. 1-7, 2017.

[12] M. A. F. Kandil and A. O. Elnady, ‘‘CFD analysis of GOE-387 airfoil,’’ *IOSR Journal of Mechanical and Civil Engineering*, vol. 14, no. 5, pp. 80-85, 2017.

[13] M. Kevadiya, ‘‘Performance of GOE-387 airfoil using CFD,’’ *International Journal of Engineering Trends and Technology*, vol. 4, no. 5, pp. 2041-2043, 2017.

[14] J. Winslow, H. Otsuka, B. Govindarajan, and I. Chopra, ‘‘Basic understanding of airfoil characteristics at low Reynolds number (10^4-10^5),’’ *Journal of Aircraft*, vol. 55, no. 3, pp. 1050-1061, 2018.

[15] N. Cao, D. S.-K. Ting, and R. Carriveau, ‘‘The performance of a high-lift airfoil in turbulent wind,’’ *Wind Engineering*, vol. 35, no. 2, pp. 179-196, 2011.

[16] E. Livya, G. Anitha, and P. Valli, ‘‘Aerodynamic analysis of dimple effect on aircraft wing,’’ *International Journal of Aerospace and Mechanical Engineering*, vol. 9, no. 2, pp. 350-353, 2015.

[17] D. Srivastav, ‘‘Flow control over airfoils using different shaped dimples,’’ International Conference on Fluid Dynamics and Thermodynamics Technologies, Singapore, 2012, pp. 92-97.

[18] A. Y. Manda and G. Satish, ‘‘Comparative study of different pipe geometries using CFD,’’ *Materials Today*, vol. 25, no. 1, pp. 25-30, 2020.

[19] G. Satish and K. A. Kumar, ‘‘Comparison of flow analysis of a sudden and gradual change of pipe diameter using fluent software,’’ *International Research Journal of Engineering and Technology*, vol. 2, no. 12, pp. 41-45, 2013.

[20] A. Y. Manda and G. Satish, ‘‘Flow behaviour on elbow with various geometries of nozzle,’’ *I-manger's Journal on Mechanical Engineering*, vol. 9, no. 2, pp. 43-51, 2019.

[21] A. R. Elbakheit, “Factors enhancing aerofoil wings for wind energy harnessing in buildings,” *Building Services Engineering Research & Technology*, vol. 35, no. 4, pp. 417-437, 2014.